# Roles of Flexible Chains in Organic Semiconducting Materials

Ting Lei, Jie-Yu Wang,* and Jian Pei*

Beijing National Laboratory for Molecular Sciences, The Key Laboratory of Bioorganic Chemistry and Molecular Engineering of Ministry of Education, College of Chemistry and Molecular Engineering, Peking University, Beijing 100871, China

ABSTRACT: In the past couple of years, remarkable progress has been made in solution-processable organic semiconducting materials for optoelectronics. The development of novel π-conjugated backbones has always been the central issue in this field. In contrast, flexible side chains are less developed and usually used only as solubilizing groups. In this Perspective, we highlight the effects of the flexible chains in organic semiconductors, including the influences of length, odd−even effect, substitution position, terminal groups, branching position, and chirality of alkyl chains, as well as some significant features of oligo(ethylene glycol) and fluoroalkyl chains. Although the roles of flexible chains in organic semiconducting materials are complex and differ when corresponding conjugated skeleton changes, in this Perspective, we emphasize the synergy of conjugated backbones and flexible side chains, which might significantly facilitate the understanding of the roles of flexible chains in structure−property relationship and promote the development of high-performance organic semiconductors.

KEYWORDS: *organic materials, organic semiconducting materials, flexible chain effect, alkyl chain effect*
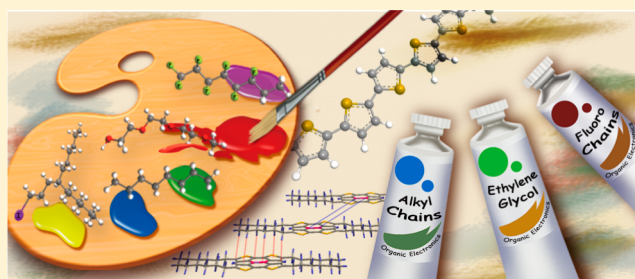
1. INTRODUCTION

As the promising materials for the next generation of electronics, such as displays, thin-film transistors, solar cells, sensors, and logic circuits, organic semiconductors have attracted broad attention from both industry and academia.[1] Solution-processablilty is one of the most attractive features of organic semiconductors, enabling low-cost, low-temperature, and large-area device fabrication.[2] To date, a large number of organic semiconductors have been developed to improve the device performance, where most of the efforts focused on the design and synthesis of new π-conjugated backbones.[3] However, strong $\pi-\pi$ interactions in organic π-conjugated systems significantly decrease their solubility, and thus flexible side chains are usually introduced to afford satisfactory solubility for purification and device fabrication.

Alkyl chains, oligo(ethylene glycol) chains, and fluoroalkyl chains are three commonly used side chains in organic semiconductors. As insulating parts, these chains generally do not directly contribute to charge transport in organic semiconductors. However, more and more studies have demonstrated the substantial impact of the flexible chains on the device performance of organic semiconductors. Some results have also indicated that even a subtle change of the flexible chains may result in a great influence on device performance.[4] In this Perspective, we highlighted recent investigations on the roles of flexible chains in organic semiconductors. Since the roles of flexible chains in organic semiconductors is quite complex and highly dependent on the conjugated backbones, we only show some representative studies to illustrate the diverse and complex effect of the flexible chains. Although the effects of flexible chains and the engineering of these chains are always accompanied by the solubility factor, herein we emphasize the influences beyond the solubility, especially those on the device performances of organic semiconductors. We hope that the summary and analysis of the roles of flexible chains will contribute to a better understanding of the structure−property relationship in organic semiconductors and facilitate the design of new compounds and the improvement of their device performance.

2. ALKYL CHAINS

Alkyl chains are the most widely used solubilizing groups in organic materials.[3b] Two factors may contribute to the dissolution of the organic materials after introducing alkyl chains: first, the additional van der Waals interactions between alkyl chains and solvent, which increase the total interaction energy between organic molecules and solvent; second, the vibrational motions of alkyl chains that may destroy the good molecular arrangement in solid state, which decrease the interactions between π-conjugated systems. Competition between solute−solute and solute−solvent interactions determines the equilibration of crystallization and dissolution, therefore controlling the self-assembly of organic semiconductors and their properties.

2.1. Length Effects of Alkyl Chains. The first organic field-effect transistor (OFET) fabricated in 1986 was based on polythiophene.[5] The hole mobility of the device is as low as 10^{-5} cm^2 V^{-1} s^{-1} due to the poor quality of the film prepared by electrochemical polymerization. To improve the film quality, alkyl chains were introduced, and a high hole mobility up to 0.1 cm^2 V^{-1} s^{-1} was achieved in edge-on packed regioregular poly(3-hexylthiophene) (**P3HT**).[6] Babel and Jenekhe reported the dependence of carrier mobility on the length of the alkyl chains in regioregular poly(3-alkylthiophene)s (**P3ATs**) (Figure 1).[7] They found that the hole mobilities of **P3AT**
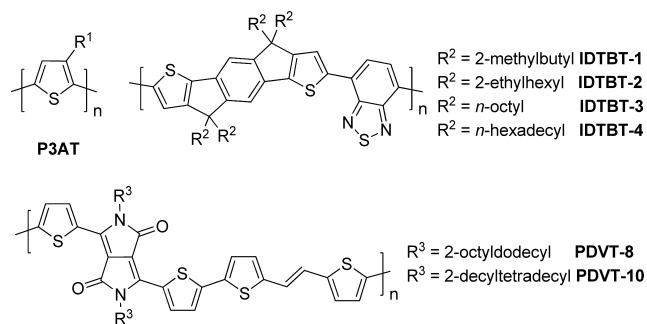

Figure 1. Organic semiconductors with various lengths of alkyl chains.

generally decreased with the increase of the chain length; for example, poly(3-butylthiophene) (**P3BT**) exhibited a hole mobility of 1.5×10^{-3} cm^2 V^{-1} s^{-1}, whereas poly(3-dodecylthiophene) gave a much lower mobility of 3.3×10^{-5} cm^2 V^{-1} s^{-1}. In addition, **P3HT** with hexyl groups gave the best device performance with a hole mobility of 0.02 cm^2 V^{-1} s^{-1}. Their results indicated that the hexyl chain is the optimum for charge transport due to the better self-organization in **P3HT**.

The effect of alkyl chain length in **P3ATs** was also observed in organic photovoltaics (OPVs). Gadisa et al. reported the morphological, bipolar carrier transport, and photovoltaic characteristics of (**P3AT**):[6,6]-phenyl-C61-butyric acid methyl ester (**PCBM**) blends.[8] Solar cells with active layers of **P3BT:PCBM**, poly(3-pentylthiophene) (**P3PT**):**PCBM**, and **P3HT:PCBM** showed power conversion efficiencies (PCEs) of 3.2, 4.3, and 4.6%, respectively. In these blends, they observed similar order of photocurrent yields and very close open circuit voltage irrespective of side-chain length, and the main source of different device performances came from fill factor values. This result was explained by the morphological changes that longer alkyl chains led to increased degree of phase separation.

Besides **P3HT**, in other polymer systems, optimizing the alkyl chain length can also effectively improve the device performance for both FETs and solar cells. For example, for polymers **IDTBT-1** to **IDTBT-4**, those with longer alkyl chains (branched or linear) exhibited higher hole mobilities (Figure 1).[9] However, their solar cell devices did not show any consistent device performance: **IDTBT-2** with longer branched alkyl chains outperformed all other polymers, whereas **IDTBT-3** with shorter linear alkyl chains gave higher PCE than **IDTBT-4**. A recent work by Liu et al. reported that the length of alkyl chain could affect the interchain $\pi-\pi$ stacking distance of conjuagted polymers.[10] **PDVT-10** with 2-decyltetradecyl side chains exhibited a remarkably high hole mobility up to 8.2 cm^2 V^{-1} s^{-1}, two times higher than that of **PDVT-8** with 2-octyldodecyl chains. The enhanced hole mobility of **PDVT-10**

was attributed to its shorter $\pi-\pi$ stacking distance (3.66 Å) than that of **PDVT-8** (3.72 Å) (Figure 1).

Organic semiconductors containing B–N subunit can afford additional intermolecular dipole–dipole interactions, thus providing a novel approach to the molecular engineering of organic semiconductors. Two azaborine compounds, **BN-TTN-C3** and **BN-TTN-C6**, with different alkyl chain lengths were recently synthesized through an efficient one-pot electrophilic borylation method (Figure 2).[11] **BN-TTN-C3** with shorter
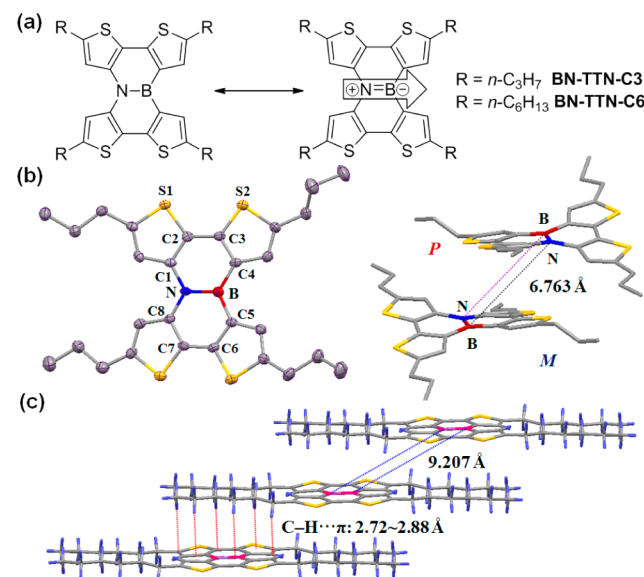

Figure 2. (a) Chemical structures of **BN-TTN-C3** and **BN-TTN-C6**. (b) Single crystal structure and molecular packing of **BN-TTN-C3**. (c) Single crystal packing of **BN-TTN-C6**. Reproduced with permission from ref 11. Copyright 2013 WILEY-VCH Verlag GmbH & Co.

alkyl chains have obviously stronger B–N dipole–dipole interactions in single crystal, and the adjacent molecules showed opposite B–N dipole moment. However, the B–N dipole interations in **BN-TTN-C6** were weakened due to the larger intermolecular distances caused by long alkyl chains, resulting in a disordered orientation of BN dipoles arrangement. Devices based on **BN-TTN-C3** revealed a hole mobility up to 0.15 cm^2 V^{-1} s^{-1}, almost 1 order of magnitude higher than that of **BN-TTN-C6** (0.03 cm^2 V^{-1} s^{-1}). Such difference in device performance was largely explained by the different crystal packings caused by the different length of alkyl chains. From the crystallographic perspective, the main driving force from a crystal structure is close packing of organic molecules.[12] For organic semiconducting molecules, both the aromatic skeleton and alkyl chains contribute to the close packing. Hence, changing the length of alkyl chains of molecules with the same aromatic skeleton will also change the van der Waals interactions and the packing level, thus allowing the modulation of the intermolecular interactions in organic semiconductors which may ultimately lead to different device performance.

2.2. Odd−Even Effects of Alkyl Chains. The earliest observation of the odd–even effect of alkyl chains was probably in the study of fatty acids in 1877.[13] The melting points of the fatty acids do not show a monotonic increase with increasing the chain length as do their boiling points. This phenomenon was also observed in *n*-alkanes, as well as for most of the terminally substituted *n*-alkane derivatives. Single crystal analysis showed that the odd–even effect in these derivatives
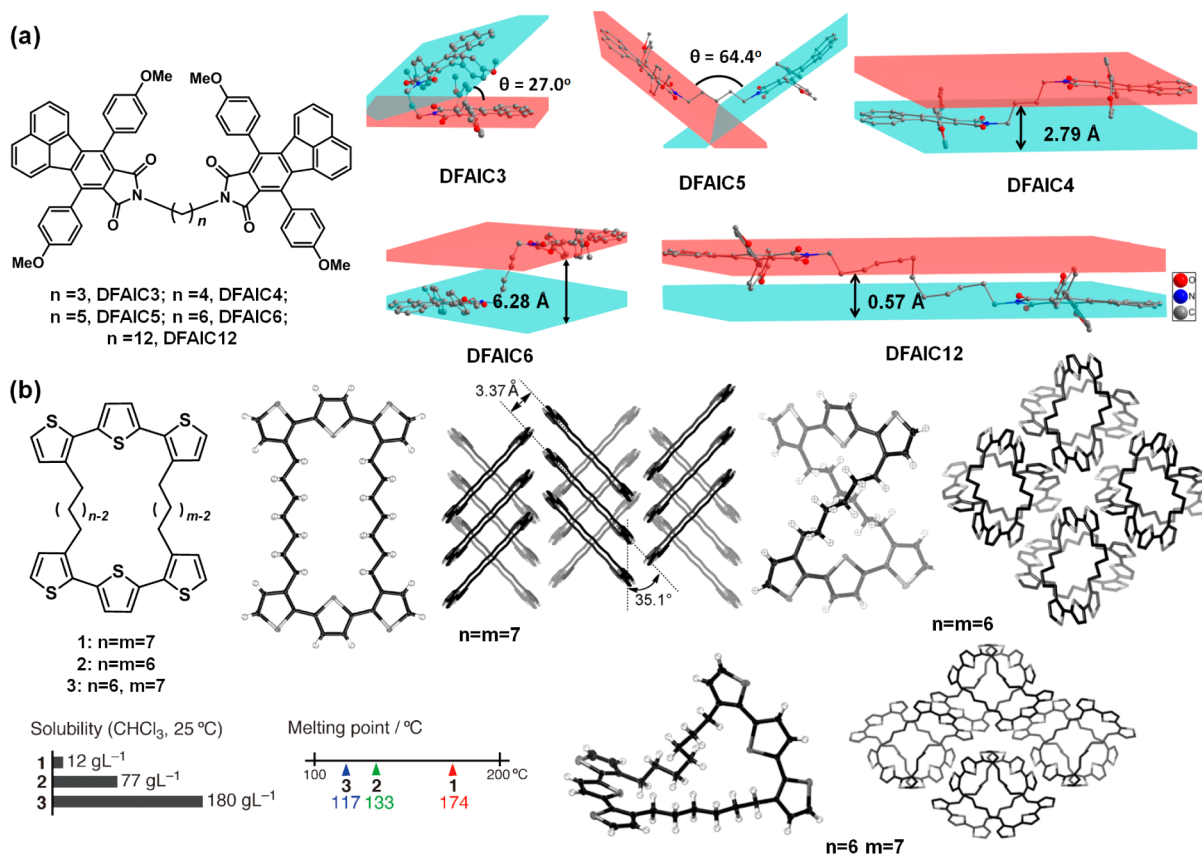
Figure 3. (a) Chemical and single crystal structures of **DFAI** with various lengths of alkyl chains. (b) Chemical and single crystal packings of three macrocycles linked by alkyl chains with different lengths. Reproduced with permission from ref 16. Copyright 2012 WILEY-VCH Verlag GmbH & Co.

strongly correlated with their solid-state packing. Even-numbered *n*-alkanes have optimal intermolecular contacts at both ends, whereas the odd-numbered ones possess these only at one end, and the distances are longer at the other end.[14] This leads to a less dense packing for the odd *n*-alkanes and thereby lower melting points. These features observed in alkanes and related compounds could also be introduced into organic semiconductors.

The odd−even effect also exerts its influence on crystal packing and charge transport after being attached onto aromatic cores. In the investigation of a series of the dimers of fluoranthene-fused imides (**DFAIs**), we found that molecules with odd carbon numbers of alkylene chains displayed stronger one-dimensional growing tendency and better crystallinity than those with even carbon numbers (Figure 3a).[15] Dimers with odd-numbered alkylene chains, such as **DFAI-C3** and **DFAIC5**, exhibited "V"-shaped molecular configuration in single crystals, whereas those with even numbers (**DFAI-C4**, **DFAI-C6**, and **DFAI-C12**) showed "Z"-shaped molecular configuration. Clearly, the zigzag conformation of alkylene chains is inherited into the molecular geometry of the dimers. Thus, the conformation of alkylene chains dominated the crystal growth, presumably due to the weak π−π interactions in this system.

Odd−even effect is also used to tune the molecular conformation of macrocycles and their crystal packings by connecting two π-conjugated skeletons with flexible alkylene linkers (Figure 3b).[16] For symmetrically connected macrocycles (*n* = *m*), different molecular conformations are obtained for odd- and even-numbered alkylene linkers. The heptylene

linkers take all *anti*-conformations, whereas among the five methylene−methylene bonds in each hexylene chain, one bond takes a *gauche* conformation. Unsymmetrically connected macrocycles formed similar twisted structures. The structural features observed for these macrocycles demonstrated that the macrocyclic restriction caused by the flexible alkylene chains significantly impacted on the intramolecular arrangement of π-skeletons, thereby leading to different crystal packing. The distinct molecular arrangements caused totally different properties from one another, including solubility, melting point, and photophysical properties in solid state, though all compounds consisted of identical π-conjugated skeletons and similar alkylene chains.

In the investigation of thienoacene-based molecules,[17] Takimiya et al. developed a series of 2,7-dialkyl substituted BTBT molecules C$_n$-BTBT for solution-processable OFETs.[18] They introduced two solubilizing alkyl groups in the molecular long-axis direction of the core to facilitate lateral intermolecular interaction (Figure 4). For *n* = 5−9, the molecules showed increased solubility in CHCl$_3$ as increasing the alkyl chain length. However, after *n* > 10, the molecules showed obviously decreased solubility in CHCl$_3$, and the solubility further decreased with increasing length of solubilizing chains. This result may be due to the increased van der Waals interactions between alkyl chains and the decreased solubility of the longer alkyl chains in CHCl$_3$. Solution-processed FET devices based on these BTBT derivatives all showed hole mobility over 0.1 cm^2 V^{-1} s^{-1}. For *n* = 5−10, the hole mobilities of derivatives with even-numbered chains outperformed those derivatives
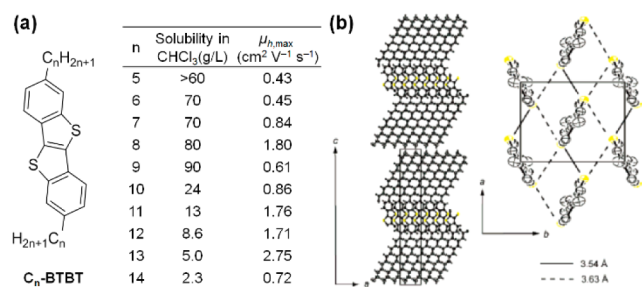
Figure 4. (a) Molecular structures, solubility in chloroform, and device performances of **C$_n$-BTBT**. (b) Single crystal packing of **C$_{12}$-BTBT**. Reproduced with permission from ref 18. Copyright 2007 from American Chemical Society.

n	Solubility in CHCl$_3$(g/L)	$\mu_{h,max}$ (cm^2 V^{-1} s^{-1})
5	>60	0.43
6	70	0.45
7	70	0.84
8	80	1.80
9	90	0.61
10	24	0.86
11	13	1.76
12	8.6	1.71
13	5.0	2.75
14	2.3	0.72

with odd-numbered chains, but the trend was reversed for n = 10−14. Obviously, the hole mobilities in these materials were affected not only by the odd−even effect but also by the length effect of the flexible chains. Both effects influence the molecular packing and charge transport. The above results indicate that odd−even effects have significant influence on molecular conformation and crystal packing though they are always accompanied by the length effects. Since molecular symmetry plays a vital role in single crystal packing, odd−even effects probably originate from the different symmetry of alkyl chains with odd and even carbon numbers.

2.3. Effects of Substitution Position. In conjugated polymers, the intrachain transport is realized by π-electron delocalization of long polymer backbones, which is largely limited by the effective conjugation length of the polymer. Since the effective conjugation length is limited by the torsional disorder along the polymer backbone,[19] substitution position of alkyl chains can exert its influence on carrier mobilities through tuning the steric hindrance effect or rotational angles. As shown in Figure 5, **PTBzT-1** and **PTBzT-2** have identical donor−acceptor polymer backbone, but with dodecyl chains attached
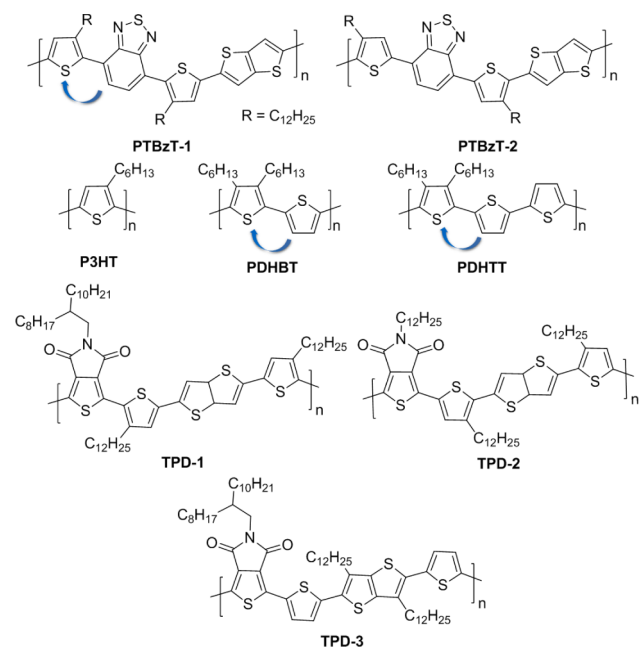

Figure 5. Investigation of the substitution position of alkyl chains in conjugated polymers; blue arrows indicate the rotational angles caused by the alkyl chains.

at different positions.[20] In **PTBzT-1**, alkyl chains were introduced near the phenyl−thienyl connecting position, which caused obviously steric repulsion and thereby increased the dihedral angles in solid state. However, **PTBzT-2** has more planar backbones, and the small rotational angles caused by the dodecyl chains were suppressed when going into solid state. **PTBzT-2** showed hole mobilities up to 5 × 10^{-4} cm^2 V^{-1} s^{-1}, whereas **PTBzT-1** only gave a hole mobility of 1 × 10^{-5} cm^2 V^{-1} s^{-1}. This result can be explained by the different steric hindrance caused by the alkyl chains. However, rotational angles caused by alkyl chains do not always degrade the device performance of polymers. For example, Bao et al. synthesized **PDHBT**, an isomer of **P3HT**, for polymer FETs and solar cells.[21] In **PDHBT**, larger backbone twisting is found to increase the ionization potential (IP) and V_{OC} in solar cells. In addition, reducing the average number of electron-donating alkyl substituents per thiophene ring also contributed to the increase of V_{OC} in **PDHTT**. There, although excessive backbone twisting resulted in a reduced J_{SC} and fill factor due to an increase of the band gap and lower hole mobility, a balance between these factors was reached with **PDHTT**, resulting in a higher PCE than **P3HT** when using **PCBM** as the acceptor.

Substitution position of alkyl chains affects the orientation of alkyl chains in solid state. Li et al. reported three thieno[3,4-c]pyrrole-4,6-dione (**TPD**)-based polymers with two dodecyl chains substituted at different positions.[22] Their experimental results showed that the alkyl chain orientations strongly affected the molecular packing pattern and the device performance. The highest hole mobility up to 1.29 cm^2 V^{-1} s^{-1} was obtained in **TPD-3**, whereas **TPD-1** and **TPD-2** only showed hole mobilites of 0.15 and 1.1 × 10^{-2} cm^2 V^{-1} s^{-1}, respectively. They proposed that the large space between the clusters of the alkyl side chains for **TPD-3** facilitated the interdigitations of the side chains and the formation of lamellar stacking structures, which contributed to the significantly higher device performances. Furthermore, several investigations showed that the substitution position of alkyl chains also played an important role in the intercalation between polymers and small molecules, such as **PCBM**, possibly due to the different size of spaces formed among the polymer side chains in solid state.[23]

Substitution position also affects the interchain π−π stacking and thereby charge transport in conjugated polymers. In the single crystal of n-hexane,[14] the shortest C−C distance (3.623 Å) comes from the methyl C atoms of adjacent columns, and the shortest distance between parallel packed alkyl chains is 4.065 Å. These distances are obviously larger than the typical π−π stacking distances (3.3−3.6 Å) found in many organic semiconductors.[3b] Thus, the alkyl chain packing in organic semiconductors may sometimes impede the π−π stacking of aromatic cores. For example, in those polymers with each unit substituted with one alkyl chain, steric hindrance may occur as indicated by the red circle in Figure 6a. To avoid the steric hindrance, a strategy named "molecular docking" was proposed in the design of polymer FETs.[24] Figure 6b illustrates the concept of the molecular docking, where the small units in conjugated polymers can dock into the cavity formed by the relatively larger aromatic cores and the branched alkyl chains. Using this strategy, isoindigo-based polymers **IIDDT** exhibited high hole mobilities up to 1.06 cm^2 V^{-1} s^{-1},[24,25] whereas **IIDDT-Me** with the identical backbone only showed the highest hole mobility of 0.11 cm^2 V^{-1} s^{-1}. This result was
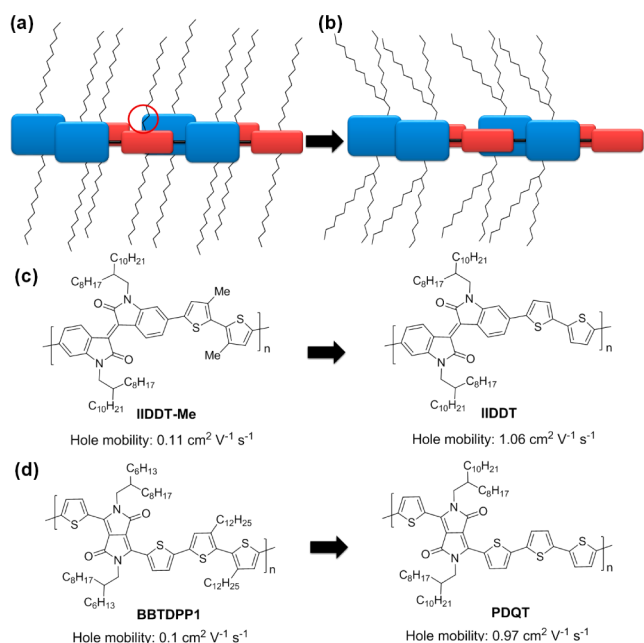
Figure 6. (a) Steric hindrance may exist when polymers are stacked with each other (red circle); (b) proposed interchain docking model to avoid the side chain impediments. Examples of alkyl side chain impediment in (c) isoindigo-based polymers and (d) DPP-based polymers.

Figure 7. SEM images of **TrO1**, **TrO2**, and **TrO3** microstructures formed from THF, dioxane, and *n*-hexane (scale bars: 10 μm). Reproduced with permission from ref 28. Copyright 2008 WILEY-VCH Verlag GmbH & Co.

largely explained by the steric hindrance effect caused by the methyl groups. Similar results were also observed in the diketopyrrolopyrrole (DPP) based polymers. With an identical backbone to **PDQT**[26] yet two additional dodecyl chains, **BBTDPP1** showed hole mobility as high as 0.1 cm^2 V^{-1} s^{-1},[27] almost 1 order of magnitude lower than that of **PDQT** (Figure 6d).

Another effect of changing the substitution position of alkyl or alkoxyl chains comes from their weak electron donating properties, which sometimes exhibits strong influence on intermolecular interactions. Three similar truxenone molecules, **TrO1**, **TrO2**, and **TrO3**, were synthesized to investigate both the effects of the substitution position and the number of alkyl chains (Figure 7).[28] **TrO2** readily dissolves in CHCl$_3$ and exhibited a melting transition at 128 °C; however, as the isomer **TrO1** has poor solubility in CHCl$_3$ and a higher melting point at 179 °C. With more alkoxyl substituents, **TrO3** showed better solubility and no T_g and T_m were observed above 50 °C. After heating their THF solution and then cooling down, only **TrO1** formed one-dimensional (1D) microwires. Upon changing to the moderately polar solvent dioxane, similar results were obtained for **TrO1**, and uniform microwires of **TrO2** and **TrO3** clearly emerged. After further decreasing the solvent polarity to *n*-hexane, no assembly structure of **TrO1** was observed due to its poor solubility. In contrast, microwires of **TrO2** not only grew longer but also tended to be more rigid and straight. However, irregular structures for **TrO3** were again observed in *n*-hexane. These results suggest that different substitution positions and numbers of alkyl chains can lead to different intermolecular interactions. Molecular calculations demonstrated that for **TrO3** the steric repulsion between the two adjacent side chains forced the alkoxyl chains to flip out of the molecular plane and increased the solubility of **TrO3**. For **TrO1** and **TrO2**, it was found that the quadruple moment of **TrO1**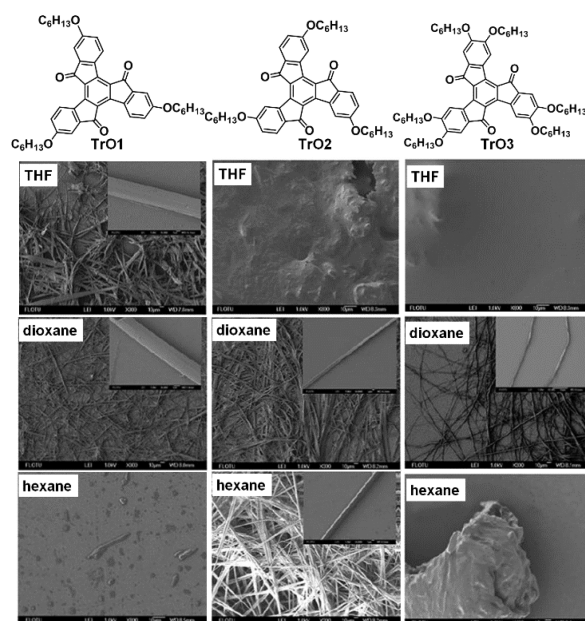 was about 50% larger than that of **TrO2** due to different substitution positions, suggesting a much stronger electrostatic interaction in **TrO1**. Thus, **TrO1** exhibited worse solubility and higher melting point, and a polar solvent such as THF should be employed to provide sufficient solubility for initiating the 1D self-assembly of **TrO1**.

2.4. Chain-End Functionalized Alkyl Chains. It has been well recognized that end-functionalized side chains can modulate the carrier injection of organic semiconductors. We introduced various functional groups, including electron-rich carbazole and electron-deficient 1,2,4-triazole and 2,5-diphenyl-1,3,4-oxadiazole, onto the side chains of organic blue emitters.[29] With these "antenna" groups, the hole/electron injection barrier of single-layer organic light-emitting diodes (OLEDs) was reduced by using electron-rich/electron-deficient groups.

Water/alcohol soluble conjugated polymers are an important class of side-chain-end functionalized polymers, which can be processed from water or other polar solvents for interface modification of organic electronics.[30] For example, using **PFN**, a side-chain-end functionalized polymer, as the injection layer in OPVs, the PCE of **PTB7** was significantly increased from 7.13% to 8.22% in a conventional device structure[31] and then was further increased to 9.21% when using an inverted device structure containing **PFN** as electron transporting layer (Figure 8a).[32] Apart from neutral functionalities, ionic functionalities are also frequently used in organic semiconductors. Conjugated polyelectrolytes (CPEs), which are conjugated polymers with pendant groups bearing ionic functionalities, exemplify the successful application of the chain-end functionalization. CPEs are widely used as the interfacial layer materials in organic electronic devices, such as OLEDs,[33] OFETs,[34] and OPVs.[35] Besides interfacial layer engineering, CPEs were also used as the active layer in organic electronics. Recently, Bazan et al. developed a low bandgap CPE, **PCPDTBT-Pyr$^+$BIm4$^-$**, for OFETs. Compared with *p*-type **PCPDTBT-Br**, **PCPDTBT-Pyr$^+$BIm4$^-$** unexpectedly exhibited *n*-type transporting behaviors, thus providing interesting properties for CPEs.
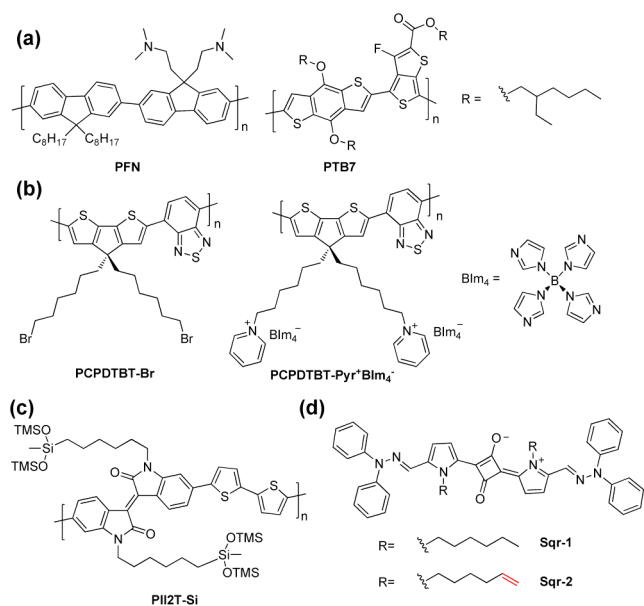
Figure 8. Chain-end functionalized organic semiconductors.

Using siloxane-terminated alkyl side chains, Bao et al. designed an isoindigo-based polymer **PII2T-Si**.[36] With such side chains, the polymer exhibited closer backbone packing and increased hole mobility up to 2.48 cm^2 V^{-1} s^{-1} (Figure 8c). The siloxane groups bring great solubility to the conjugated polymers, critical for the good processability in device fabrication. Using the same concept, Yang and Oh et al. reported the use of the siloxane-terminated side chains for DPP–polymers and obtained high hole mobilities up to 3.97 cm^2 V^{-1} s^{-1} and electron mobilities up to 2.20 cm^2 V^{-1} s^{-1}.[37]

Sometimes, a subtle change in the terminal of alkyl chains could greatly affect the molecular packing and device performance not only in FETs but also in solar cells. For example, the only difference in **Sqr-1** and **Sqr-2** is the terminal of side chains (Figure 8d).[38] However, **Sqr-2** exhibited closer π−π stacking between adjacent molecules, thereby leading to a better device performance (PCE: 2.05%) than that of **Sqr-1** (PCE: 1.47%) in BHJ solar cells.

2.5. Branched Alkyl Chains and the Influence of the Branching Point. Besides providing better solubility for conjugated polymers, branched alkyl chains also affect the polymer packing in bulk heterojunction solar cells. In the investigation of alkyl chain effect in **PBDTTPD** polymers (Figure 9a),[39] Beaujuge et al. found that replacing the branched side chains by linear ones on the BDT motifs induced a critical change in polymer packing in thin films. For the polymers with identical R$_2$ groups (R$_2$ = C8), the polymer with **2EH** alkyl chains preferred to adopt a "face-on" orientation, whereas the polymer with **C14** chains showed a nearly isotropic molecular packing without a preferential "face-on" orientation. The polymer with **2EH** chains showed obviously higher PCE (7.5%) than those with linear chains (**C14**: 4.1%; **C12**: 3.2%), which was consistent with the fact that predominantly "face-on" polymer commonly associated with higher solar cell performance.[40] In addition, the length effect of alkyl chain on solar cell performance was also investigated in this system. For polymers with various alkyl chain lengths in the R$_2$ group (R$_1$ = **2EH**), the polymer with **C7** chain gave the best performance with PCE up to 8.5%; however, **C6** and **C8** chains gave relatively lower results.
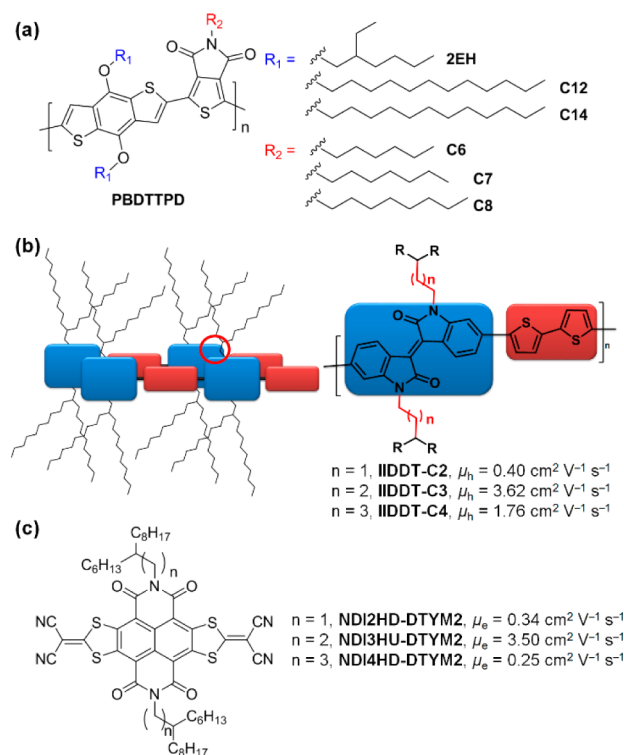

Figure 9. Polymers and small molecules with branched alkyl chains and the influence of the branching position on their device performance.

Compared with linear alkyl chains, branched alkyl chains, such as 2-ethylhexyl, 2-octyldodecyl, and 2-decyltetradecyl groups, can provide better solubility for conjugated polymers. Interestingly, only alkyl chains branched at the second position are commonly used in organic semiconductors, presumably because they are readily available. With these branched chains, the distance between the branching points and the conjugated backbone is merely one methylene group. Similar to the impediment of alkyl chains in Figure 6a, steric hindrance may also occur when the branching point of alkyl chains is close to polymer backbones (Figure 9b).

To avoid such steric hindrance effect, Bao et al. developed unconventional siloxane-terminated alkyl side chains (Figure 8c). However, because the trimethylsilyl group cannot survive certain reaction conditions, the application of this elegantly designed group is limited. On the other hand, the structural difference between siloxane-terminated chains and conventional branched alkyl chains is drastic, thus prohibiting a deep insight into the underlying structure−property relationship. On the basis of these considerations, we designed three novel branched alkyl chains (3-decyltridecyl, 4-decyltetradecyl, and 5-decylpentadecyl) to modify the isoindigo-based polymer to investigate how moving the branching point of these "more conventional" alkyl chains farther from the backbone influences the mobilities (Figure 9b).[4] **IIDDT-C3** exhibited the highest hole mobility up to 3.62 cm^2 V^{-1} s^{-1} after thermal annealing, significantly higher than that of **IIDDT**. **IIDDT-C4** also displayed increased mobility, and the highest mobility was 1.76 cm^2 V^{-1} s^{-1}. However, **IIDDT-C2** showed decreased device performance, and its highest mobility was only 0.40 cm^2 V^{-1} s^{-1}. After moving the branching point away from the backbones, the polymers showed gradually decreased π−π stacking distances: 3.75 Å for **IIDDT**, 3.61 Å for **IIDDT-C2**, and 3.57 Å for both

IIDDT-C3 and **IIDDT-C4**. Thus, the largely improved mobilities are likely due to the decreased π–π stacking distances. Previous results have shown that the mobilities of conjugated polymer increased with decreasing the interchain π–π stacking distances. However, in our system, the mobilities of the polymers did not always increase with the decrease of the π–π stacking distances. Such inconsistency between device performances and π-stacking distances was probably caused by the different stacking conformations of the four polymers, which also played vital roles in interchain carrier transport. Furthermore, we successfully applied these "farther branched alkyl chains" in both ambipolar and *n*-type conjugated polymers and obtained high hole or electron mobilities, demonstrating their broad applications in organic electronics.[41]

The roles of both length and branching position of alkyl chains were recently investigated in a series of naphthalene diimides (NDI)-based *n*-type small-molecule semiconductors (Figure 9c).[42] In this system, the authors found that changing the length of alkyl chains had a moderate influence on thin film microstructures and only resulted in limited effects on device performance. However, modulating the branching position of alkyl chains resulted in dramatic differences in electron mobilities though only subtle changes in molecular packing were observed. Through varying the branching position of the side chains, **NDI3HU-DTYM2** exhibited the best device performance with the highest electron mobility up to 3.50 $cm^2 V^{-1} s^{-1}$, almost 1 order of magnitude higher than those of its counterparts with other branched alkyl chains. These results demonstrated that the variation of the branching point of alkyl chain is a powerful strategy to modulate the intermolecular interactions and device performance in organic semiconductors.

2.6. Chirality of Branched Alkyl Chains. Chirality has been widely investigated in the research of natural products and drugs, as well as supramolecular systems. Stereoisomers and their mixtures usually exhibit different crystal structures and thereby different solid-state properties. By using the chiral alkyl side chains, circularly polarized electroluminescence (CPEL) was first demonstrated in poly(phenylene vinylene) derivatives (PPVs).[43] These devices emitted light with the right-handed emission intensity slightly larger than the left-handed intensity. To increase the dissymmetry factor in electroluminescence, chiral alkyl chain substituted polyfluorenes (**PFs**) were used as the active layer (Figure 10a).[44] Strong circular dichroic (CD) signals were observed from the films of **PF-1** and **PF-2**.
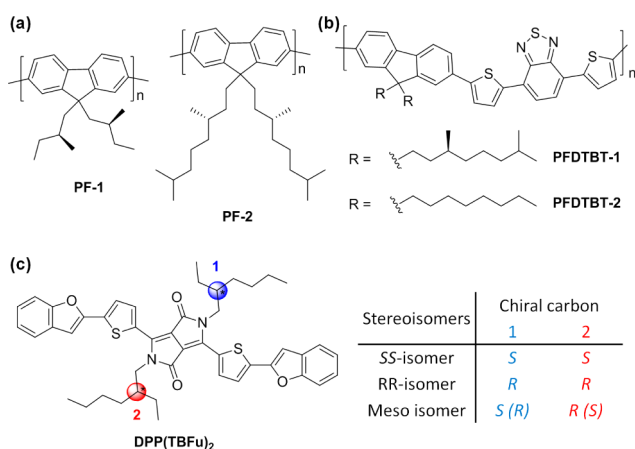
However, the sign of signal for **PF-1** is opposite to that for **PF-2**, though they both have alkyl chains with *S*-chirality. Such difference in the CD signals might be attributed to the different distances of the chiral center in the side chain to the backbone. **PF-2** emitted strong circularly polarized light with dissymmetry factor up to 0.25, almost 200 times larger than above-mentioned PPVs.

Polymers with chiral side chains can show a large difference in absorbance of *L* and *R* circular polarized light in solid state,[45] which is related to the presence of a liquid crystalline state, presumably of cholesteric nature.[46] Thus, they might be useful for constructing photodiodes or OPVs that are sensitive to the circular polarization of light. Meskers et al. reported their investigation of OPVs based chiral **PFDTBT-1** and achiral **PFDTBT-2** by using a bilayer device configuration. Compared with those of achiral **PFDTBT-2**, photovoltaic devices based on **PFDTBT-1** exhibited different short-circuit photocurrent for *L* and *R* polarized incident light. Interestingly, the devices of **PFDTBT-1** illuminated with left circular polarized light that was less absorbed produced a higher photocurrent. This counterintuitive observation can be explained by the effective utilization of the left light at the polymer/C_{60} interface due to the lower probability of the absorption of the left light in the polymer layer when light passes through the polymer layer.

Asymmetrical branched alkyl chains, such as 2-ethylhexyl group, are widely used in organic semiconductors. Clearly, the as-synthesized conjugated molecules will consist of a mixture of stereoisomers due to the asymmetrical substitutions of alkyl chains. To investigate the stereoisomerism effects of alkyl chains, three stereoisomers of **DPP(TBFu)₂**, meso isomer, *RR*-isomer, and *SS*-isomer, were isolated.[47] The *RR*- and *SS*-isomer, which are enantiomers, showed very similar crystal structures, thin-film morphologies, and FET properties. The meso isomer showed the highest carrier mobility among the stereoisomers and the as-synthesized isomeric mixture, due to its better π–π stacking and shorter plane-to-plane distance in single crystal. Furthermore, the single crystal of isolated isomers were found to be obtained more easily than the mixture. Thus, modulating the chirality of alkyl chains is also an effective approach to improve the device performance of organic semiconductors.

3. OLIGO(ETHYLENE GLYCOL) CHAINS

Compared with hydrophobic alkyl chains, one of the most important characteristics of the oligo(ethylene glycol) chains is their hydrophilic property due to many ether groups. Although oligo(ethylene glycol) chains have been widely used to stabilize supramolecular structures,[48] their applications in organic electronic devices are rare. Aida et al. built several organic nanotubes based on hexa-peri-hexabenzocoronene (HBC) derivatives bearing both hydrophobic alkyl and hydrophilic triethylene glycol (TEG) chains (Figure 11a).[49] These molecules self-assembled into well-defined 1D bilayer tubular structures, stabilized by π–π interactions and hydrophobic interactions. In this system, a quick photoconductive response[50] and an interesting supramolecular linear heterojunction[51] were both realized. In our group, we developed a two-dimensional bilayer nanosheet constructed from a butterfly shaped molecule for free-standing-film FETs (Figure 11b).[52] This molecule processed both hydrophobic alkyl chains and hydrophilic TEG chains and formed free-standing bilayer nanosheets in solution through strong π–π stacking, assisted by van der Waals interactions of long aliphatic chains. Since the exteriors of the bilayer sheets were surrounded by TEG chains, further
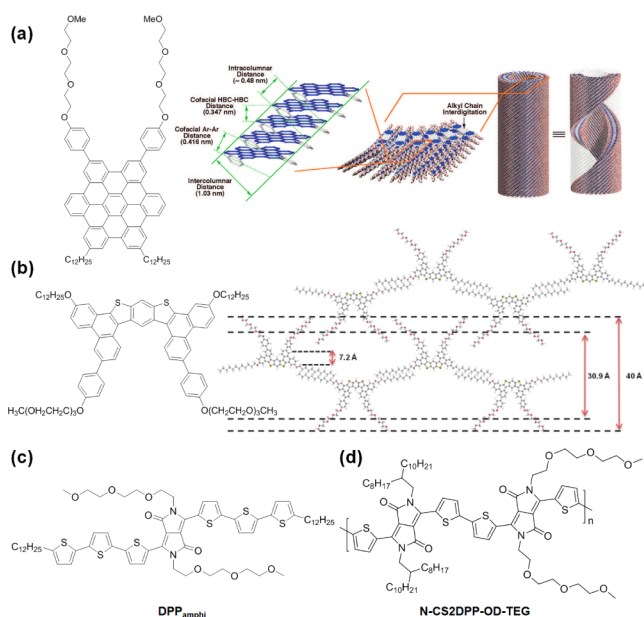
Figure 10. Polymers and small molecules with chiral alkyl chains.

(a)

(b)

(c) DPP$_{amphi}$

(d) N-CS2DPP-OD-TEG

Figure 11. (a) The amphiphilic HBC derivative and it molecular packing in nanotubes. Reproduced with permission from ref 49. Copyright 2008 from American Chemical Society. (b) The molecular structure of the butterfly shaped molecule and its proposed molecular packing in nanosheet. Amphiphilic molecules: (c) **DPP$_{amphi}$** and (d) **N-CS2DPP-OD-TEG**.

aggregation was inhibited. FET devices based on the nanosheets exhibited good device performance with hole mobility up to 0.02 cm^2 V^{-1} s^{-1}.

Besides their application in organic nano/micromaterials, oligo(ethylene glycol) chains have also attracted increasing attention in thin-film devices. Recently, an amphiphilic π-conjugated molecule **DPP$_{amphi}$** was developed by Reynolds et al. for OFETs (Figure 11c).[53] They found that **DPP$_{amphi}$** exhibited much better solubility in organic solvents when using TEG chains rather than dodecyl (C$_{12}$H$_{25}$) chains. Using the molecules with TEG chains, an average hole mobility of 3.4 × 10^{-3} cm^2 V^{-1} s^{-1} was obtained. Similar strategy was also employed in the design of a conjugated polymer **N-CS2DPP-OD-TEG**,[54] which also showed better solubility in common organic solvents when TEG chains were used (Figure 11d). The polymer exhibited high electron mobilities up to 3 cm^2 V^{-1} s^{-1}. These examples indicate that TEG chains may endow organic semiconductors with other novel properties rather than the amphiphilic one, thus demonstrating promising applications of TEG chains in the design of organic semiconductors.

4. FLUOROALKYL CHAINS

Due to the high electronegativity of fluorine atom, fluoroalkyl chains exert their electron-withdrawing ability via both electrostatic (through-space) and sigma-inductive (through-bond) effects. Oligothiophenes are mainly p-type semiconductors. However, Marks et al. prepared a series of oligothiophenes bearing fluoroalkyl chains to compare with their alkylated counterparts (Figure 12).[55] The introduction of fluoroalkyl chains improved the chemical/thermal stability, volatility, and electron affinity of oligothiophenes. The fluoroalkyl oligothiophenes behaved as n-type semiconductors whereas the alkyl-substituted oligothiophenes exhibited a p-type character as the unsubstituted oligothiophenes. For instance, α,ω-diperfluorohexyl-4T (**DFH-4T**) exhibited the highest
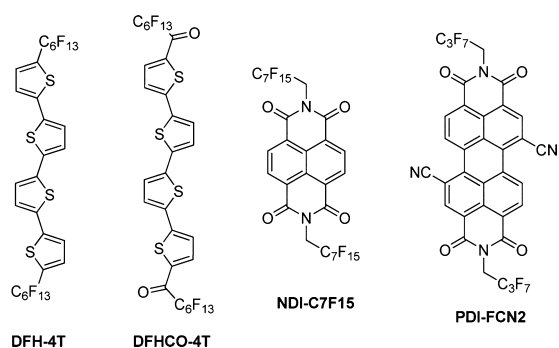

Figure 12. Some n-type organic semiconductors containing fluoroalkyl chains.

electron mobility of 0.22 cm^2 V^{-1} s^{-1}. Furthermore, they also developed a carbonyl-functionalized quaterthiophene with perfluoroalkyl chains (**DFHCO-4T**), and an electron mobility as high as 0.6 cm^2 V^{-1} s^{-1} was obtained.[56]

Apart from electron-withdrawing properties, fluoroalkyl side chains can provide a barrier to oxygen and water and stabilize electron transport in **NDI-C7F15**, due to the larger van der Waals radii of fluoroalkyl chains than their hydrocarbon counterparts.[57] By using this design strategy, Marks et al. developed **PDI-FCN2** based on perylene 3,4:9,10-tetracarboxylic diimide (PDI), which also exhibited air-stable n-type transporting behavior with electron mobilities up to 0.65 cm^2 V^{-1} s^{-1}.[58] However, such "barrier" effect of fluoroalkyl chains is still under debate. For example, Weitz et al. observed that the rate of mobility degradation in air was the same for five core-cyanated **PDIs**, irrespective of the side chains, which is inconsistent with the prediction of the "barrier" theory.[59]

The incorporation of fluorocarbon units into organic molecules can provide many advantages, such as low friction coefficient, high rigidity, extremely low surface energy, hydrophobicity, lipophobicity, chemical inertness, and thermal resistance.[60] For example, due to the lipophobicity of fluorocarbons, some π-conjugated fluorinated amphiphiles bearing both alkyl and fluoroalkyl chains exhibited various self-assembly properties in solid state.[61] However, these interesting properties of fluoroalkyl chains are less studied in organic semiconductors, thus warranting a further investigation in this field.

5. SUMMARY AND OUTLOOK

In this Perspective, using several representative examples, we summarize and discuss the influences of the length, odd−even, substitution position, end groups, branching position, and chirality of alkyl chains, as well as some significant features of oligo(ethylene glycol) and fluoroalkyl chains. These characteristics of flexible chains have exhibited nonignorable, sometimes significant, influences on the properties and device performance of organic semiconductors. Compared with the onerous design and synthesis of novel π-conjugated systems, modulating the flexible side chain appears to be a roundabout approach to obtain higher device performance for organic semiconductors. Since the device performance of organic semiconductors is highly dependent on molecular packing, film morphology, and interfacial properties, the roles of flexible chains on device performance are thus complex, which cannot be illustrated simply in one or two examples. Although in-depth understanding of the flexible chain effect needs the development of other disciplines, such as supramolecular chemistry, crystal

engineering, and physics of condensed matters, we believe that the integrated consideration and engineering of both π-conjugated backbones and flexible chains will greatly facilitate the development of organic semiconductors.

AUTHOR INFORMATION

Corresponding Author

*E-mail: jianpei@pku.edu.cn (J.P.), jieyuwang@pku.edu.cn (J.-Y.W.).

Notes

The authors declare no competing financial interest.

Biographies

Ting Lei received his B.Sc. degree in Chemistry (advisor Jian Pei) from Peking University in 2008. He continued his study in Pei's group as a Ph.D. candidate and obtained his Ph.D. degree in this July. His research includes the synthesis and characterization of organic materials for polymer FETs and solar cells and the synthesis and mechanism investigation of organic nano/micro materials.

Jie-Yu Wang is currently an Assistant Professor of Organic Chemistry in Peking University. She received her Ph.D. degree in Organic Chemistry from Peking University in 2009. Her research interests relate to organic synthesis, supramolecular chemistry, and fabrication of organic nano/micromaterials.

Jian Pei received his B.Sc. and Ph.D. degrees in Organic Chemistry from Peking University. In 1998, he joined the group of Professor A. J. Heeger to study organic semiconducting materials. He came back to Peking University in 2001 and now is a Professor in Chemistry. His research interests relate to organic synthesis, supramolecular chemistry, organic semiconductors, and optoelectronic devices.

ACKNOWLEDGMENTS

REFERENCES

(1) (a) Heeger, A. J.; Sariciftci, N. S.; Namdas, E. B. *Semiconducting and Metallic Polymers*; Oxford University Press: 2010. (b) Klauk, H. *Organic Electronics: Materials, Manufacturing and Applications*; Wiley-VCH: Weinheim: Germany, 2006. (c) Bao, Z.; Locklin, J. *Organic Field-Effect Transistors*; CRC Press: 2007.

(2) Moonen, P. F.; Yakimets, I.; Huskens, J. *Adv. Mater.* **2012**, *24*, 5526−5541.

(3) (a) Mei, J.; Diao, Y.; Appleton, A. L.; Fang, L.; Bao, Z. *J. Am. Chem. Soc.* **2013**, *135*, 6724−6746. (b) Wang, C.; Dong, H.; Hu, W.; Liu, Y.; Zhu, D. *Chem. Rev.* **2012**, *112*, 2208−2267. (c) Beaujuge, P. M.; Fréchet, J. M. J. *J. Am. Chem. Soc.* **2011**, *133*, 20009−20029.

(4) Lei, T.; Dou, J.-H.; Pei, J. *Adv. Mater.* **2012**, *24*, 6457−6461.

(5) Tsumura, A.; Koezuka, H.; Ando, T. *Appl. Phys. Lett.* **1986**, *49*, 1210−1212.

(6) Sirringhaus, H.; Brown, P. J.; Friend, R. H.; Nielsen, M. M.; Bechgaard, K.; Langeveld-Voss, B. M. W.; Spiering, A. J. H.; Janssen, R. A. J.; Meijer, E. W.; Herwig, P.; de Leeuw, D. M. *Nature* **1999**, *401*, 685−688.

(7) Babel, A.; Jenekhe, S. A. *Synth. Met.* **2005**, *148*, 169−173.

(8) Gadisa, A.; Oosterbaan, W. D.; Vandewal, K.; Bolsée, J.-C.; Bertho, S.; D'Haen, J.; Lutsen, L.; Vanderzande, D.; Manca, J. V. *Adv. Funct. Mater.* **2009**, *19*, 3300−3306.

(9) Bronstein, H.; Leem, D. S.; Hamilton, R.; Woebkenberg, P.; King, S.; Zhang, W.; Ashraf, R. S.; Heeney, M.; Anthopoulos, T. D.; de Mello, J.; McCulloch, I. *Macromolecules* **2011**, *44*, 6649−6652.

(10) Chen, H.; Guo, Y.; Yu, G.; Zhao, Y.; Zhang, J.; Gao, D.; Liu, H.; Liu, Y. *Adv. Mater.* **2012**, *24*, 4618−4622.

(11) Wang, X.-Y.; Lin, H.-R.; Lei, T.; Yang, D.-C.; Zhuang, F.-D.; Wang, J.-Y.; Yuan, S.-C.; Pei, J. *Angew. Chem., Int. Ed.* **2013**, *52*, 3117−3120.

(12) (a) Desiraju, G. R. *J. Am. Chem. Soc.* **2013**, *135*, 9952−9967. (b) Gavezzotti, A. *Acc. Chem. Res.* **1994**, *27*, 309−314. (c) Kitaigorodskii, A. *Acta Crystallogr.* **1965**, *18*, 585−590.

(13) Baeyer, A. *Ber. Chem. Ges.* **1877**, *10*, 1286−1288.

(14) Boese, R.; Weiss, H.-C.; Bläser, D. *Angew. Chem., Int. Ed.* **1999**, *38*, 988−992.

(15) Ding, L.; Li, H.-B.; Lei, T.; Ying, H.-Z.; Wang, R.-B.; Zhou, Y.; Su, Z.-M.; Pei, J. *Chem. Mater.* **2012**, *24*, 1944−1949.

(16) Saito, S.; Nakakura, K.; Yamaguchi, S. *Angew. Chem., Int. Ed.* **2012**, *51*, 714−717.

(17) Takimiya, K.; Shinamura, S.; Osaka, I.; Miyazaki, E. *Adv. Mater.* **2011**, *23*, 4347−4370.

(18) Ebata, H.; Izawa, T.; Miyazaki, E.; Takimiya, K.; Ikeda, M.; Kuwabara, H.; Yui, T. *J. Am. Chem. Soc.* **2007**, *129*, 15732−15733.

(19) Grozema, F. C.; van Duijnen, P. T.; Berlin, Y. A.; Ratner, M. A.; Siebbeles, L. D. A. *J. Phys. Chem. B* **2002**, *106*, 7791−7795.

(20) Biniek, L.; Fall, S.; Chochos, C. L.; Anokhin, D. V.; Ivanov, D. A.; Leclerc, N.; Lévêque, P.; Heiser, T. *Macromolecules* **2010**, *43*, 9779−9786.

(21) Ko, S.; Hoke, E. T.; Pandey, L.; Hong, S.; Mondal, R.; Risko, C.; Yi, Y.; Noriega, R.; McGehee, M. D.; Brédas, J.-L.; Salleo, A.; Bao, Z. *J. Am. Chem. Soc.* **2012**, *134*, 5222−5232.

(22) Wu, Q.; Wang, M.; Qiao, X.; Xiong, Y.; Huang, Y.; Gao, X.; Li, H. *Macromolecules* **2013**, *46*, 3887−3894.

(23) Mayer, A. C.; Toney, M. F.; Scully, S. R.; Rivnay, J.; Brabec, C. J.; Scharber, M.; Koppe, M.; Heeney, M.; McCulloch, I.; McGehee, M. D. *Adv. Funct. Mater.* **2009**, *19*, 1173−1179.

(24) Lei, T.; Cao, Y.; Zhou, X.; Peng, Y.; Bian, J.; Pei, J. *Chem. Mater.* **2012**, *24*, 1762−1770.

(25) Lei, T.; Cao, Y.; Fan, Y.; Liu, C.-J.; Yuan, S.-C.; Pei, J. *J. Am. Chem. Soc.* **2011**, *133*, 6099−6101.

(26) Li, Y.; Sonar, P.; Singh, S. P.; Soh, M. S.; van Meurs, M.; Tan, J. *J. Am. Chem. Soc.* **2011**, *133*, 2198−2204.

(27) Bürgi, L.; Turbiez, M.; Pfeiffer, R.; Bienewald, F.; Kirner, H.-J.; Winnewisser, C. *Adv. Mater.* **2008**, *20*, 2217−2224.

(28) Wang, J.-Y.; Yan, J.; Li, Z.; Han, J.-M.; Ma, Y.; Bian, J.; Pei, J. *Chem.—Eur. J.* **2008**, *14*, 7760−7764.

(29) Lei, T.; Luo, J.; Wang, L.; Ma, Y.; Wang, J.; Cao, Y.; Pei, J. *New J. Chem.* **2010**, *34*, 699−707.

(30) Huang, F.; Wu, H.; Cao, Y. *Chem. Soc. Rev.* **2010**, *39*, 2500−2521.

(31) He, Z.; Zhong, C.; Huang, X.; Wong, W.-Y.; Wu, H.; Chen, L.; Su, S.; Cao, Y. *Adv. Mater.* **2011**, *23*, 4636−4643.

(32) He, Z.; Zhong, C.; Su, S.; Xu, M.; Wu, H.; Cao, Y. *Nat. Photon.* **2012**, *6*, 591−595.

(33) Hoven, C. V.; Yang, R.; Garcia, A.; Crockett, V.; Heeger, A. J.; Bazan, G. C.; Nguyen, T.-Q. *Proc. Natl. Acad. Sci. U.S.A.* **2008**, *105*, 12730−12735.

(34) Seo, J. H.; Gutacker, A.; Walker, B.; Cho, S.; Garcia, A.; Yang, R.; Nguyen, T.-Q.; Heeger, A. J.; Bazan, G. C. *J. Am. Chem. Soc.* **2009**, *131*, 18220−18221.

(35) Seo, J. H.; Gutacker, A.; Sun, Y.; Wu, H.; Huang, F.; Cao, Y.; Scherf, U.; Heeger, A. J.; Bazan, G. C. *J. Am. Chem. Soc.* **2011**, *133*, 8416−8419.

(36) Mei, J.; Kim, D. H.; Ayzner, A. L.; Toney, M. F.; Bao, Z. *J. Am. Chem. Soc.* **2011**, *133*, 20130−20133.

(37) Lee, J.; Han, A. R.; Kim, J.; Kim, Y.; Oh, J. H.; Yang, C. *J. Am. Chem. Soc.* **2012**, *134*, 20713−20721.

(38) Bagnis, D.; Beverina, L.; Huang, H.; Silvestri, F.; Yao, Y.; Yan, H.; Pagani, G. A.; Marks, T. J.; Facchetti, A. *J. Am. Chem. Soc.* **2010**, *132*, 4074−4075.

(39) Cabanetos, C.; El Labban, A.; Bartelt, J. A.; Douglas, J. D.; Mateker, W. R.; Fréchet, J. M. J.; McGehee, M. D.; Beaujuge, P. M. *J. Am. Chem. Soc.* **2013**, *135*, 4656−4659.

(40) (a) Piliego, C.; Holcombe, T. W.; Douglas, J. D.; Woo, C. H.; Beaujuge, P. M.; Fréchet, J. M. J. *J. Am. Chem. Soc.* **2010**, *132*, 7595−7597. (b) Kim, D. H.; Ayzner, A. L.; Appleton, A. L.; Schmidt, K.; Mei, J.; Toney, M. F.; Bao, Z. *Chem. Mater.* **2013**, *25*, 431−440.

(41) (a) Lei, T.; Dou, J.-H.; Cao, X.-Y.; Wang, J.-Y.; Pei, J. *J. Am. Chem. Soc.* **2013**, DOI: 10.1021/ja403624a. (b) Lei, T.; Dou, J.-H.; Ma, Z.-J.; Yao, C.-H.; Liu, C.-J.; Wang, J.-Y.; Pei, J. *J. Am. Chem. Soc.* **2012**, *134*, 20025−20028. (c) Lei, T.; Dou, J.-H.; Ma, Z.-J.; Liu, C.-J.; Wang, J.-Y.; Pei, J. *Chem. Sci.* **2013**, *4*, 2447−2452.

(42) Zhang, F.; Hu, Y.; Schuettfort, T.; Di, C.-A.; Gao, X.; McNeill, C. R.; Thomsen, L.; Mannsfeld, S. C. B.; Yuan, W.; Sirringhaus, H.; Zhu, D. *J. Am. Chem. Soc.* **2013**, *135*, 2338−2349.

(43) Peeters, E.; Christiaans, M. P. T.; Janssen, R. A. J.; Schoo, H. F. M.; Dekkers, H. P. J. M.; Meijer, E. W. *J. Am. Chem. Soc.* **1997**, *119*, 9909−9910.

(44) Oda, M.; Nothofer, H. G.; Lieser, G.; Scherf, U.; Meskers, S. C. J.; Neher, D. *Adv. Mater.* **2000**, *12*, 362−365.

(45) Abbel, R.; Schenning, A. P. H. J.; Meijer, E. W. *Macromolecules* **2008**, *41*, 7497−7504.

(46) Geng, Y.; Trajkovska, A.; Culligan, S. W.; Ou, J. J.; Chen, H. M. P.; Katsis, D.; Chen, S. H. *J. Am. Chem. Soc.* **2003**, *125*, 14032−14038.

(47) Liu, J.; Zhang, Y.; Phan, H.; Sharenko, A.; Moonsin, P.; Walker, B.; Promarak, V.; Nguyen, T.-Q. *Adv. Mater.* **2013**, *25*, 3645−3650.

(48) Kim, H.-J.; Kim, T.; Lee, M. *Acc. Chem. Res.* **2010**, *44*, 72−82.

(49) Jin, W.; Yamamoto, Y.; Fukushima, T.; Ishii, N.; Kim, J.; Kato, K.; Takata, M.; Aida, T. *J. Am. Chem. Soc.* **2008**, *130*, 9434−9440.

(50) Yamamoto, Y.; Fukushima, T.; Suna, Y.; Ishii, N.; Saeki, A.; Seki, S.; Tagawa, S.; Taniguchi, M.; Kawai, T.; Aida, T. *Science* **2006**, *314*, 1761−1764.

(51) Zhang, W.; Jin, W.; Fukushima, T.; Saeki, A.; Seki, S.; Aida, T. *Science* **2011**, *334*, 340−343.

(52) Yin, J.; Zhou, Y.; Lei, T.; Pei, J. *Angew. Chem., Int. Ed.* **2011**, *50*, 6320−6323.

(53) Mei, J.; Graham, K. R.; Stalder, R.; Tiwari, S. P.; Cheun, H.; Shim, J.; Yoshio, M.; Nuckolls, C.; Kippelen, B.; Castellano, R. K.; Reynolds, J. R. *Chem. Mater.* **2011**, *23*, 2285−2288.

(54) Kanimozhi, C.; Yaacobi-Gross, N.; Chou, K. W.; Amassian, A.; Anthopoulos, T. D.; Patil, S. *J. Am. Chem. Soc.* **2012**, *134*, 16532−16535.

(55) Facchetti, A.; Mushrush, M.; Yoon, M.-H.; Hutchison, G. R.; Ratner, M. A.; Marks, T. J. *J. Am. Chem. Soc.* **2004**, *126*, 13859−13874.

(56) Yoon, M.-H.; DiBenedetto, S. A.; Facchetti, A.; Marks, T. J. *J. Am. Chem. Soc.* **2005**, *127*, 1348−1349.

(57) Katz, H. E.; Lovinger, A. J.; Johnson, J.; Kloc, C.; Siegrist, T.; Li, W.; Lin, Y. Y.; Dodabalapur, A. *Nature* **2000**, *404*, 478−481.

(58) Jones, B. A.; Ahrens, M. J.; Yoon, M.-H.; Facchetti, A.; Marks, T. J.; Wasielewski, M. R. *Angew. Chem., Int. Ed.* **2004**, *43*, 6363−6366.

(59) Weitz, R. T.; Amsharov, K.; Zschieschang, U.; Villas, E. B.; Goswami, D. K.; Burghard, M.; Dosch, H.; Jansen, M.; Kern, K.; Klauk, H. *J. Am. Chem. Soc.* **2008**, *130*, 4637−4645.

(60) Scheirs, J. *Modern Fluoropolymers: High Performance Polymers for Diverse Applications*; John Wiley & Sons: New York, 1997.

(61) (a) Clark, C. G.; Floudas, G. A.; Lee, Y. J.; Graf, R.; Spiess, H. W.; Müllen, K. *J. Am. Chem. Soc.* **2009**, *131*, 8537−8547. (b) Wang, B.; Watt, S.; Hong, M.; Domercq, B.; Sun, R.; Kippelen, B.; Collard, D. M. *Macromolecules* **2008**, *41*, 5156−5165.